

# Solar thermochemical splitting of CO<sub>2</sub> into separate streams of CO and O<sub>2</sub> with high selectivity, stability, conversion, and efficiency

Daniel Marxer, Philipp Furler, Michael Takacs, Aldo Steinfeld\*

Department of Mechanical and Process Engineering, ETH Zurich, 8092 Zurich, Switzerland

## SUPPLEMENTARY INFORMATION

Figure S1 shows the nominal solar reactor temperature, total pressure, and specific O<sub>2</sub> and CO evolution rates during three CO<sub>2</sub>-splitting redox cycles, with the reduction step conducted under varying  $p_{\text{total}}$  (Fig. S1a) or  $\dot{V}_{\text{Ar}}$  (Fig. S1b) applied during the reduction step. Figure S2 shows the absolute O<sub>2</sub>/CO evolution, energy required for vacuum pumping ( $Q_{\text{pump}}$ ) and inert gas separation ( $Q_{\text{inert}}$ ), and  $\eta_{\text{solar-to-fuel}}$  as a function of  $p_{\text{total}}$  (Fig. S2a) or  $\dot{V}_{\text{Ar}}$  (Fig. S2b) applied during the reduction step. Figure S3 shows the nominal solar reactor temperature, total pressure, and specific O<sub>2</sub> and CO evolution rates for a CO<sub>2</sub>-splitting cycle with ambient air purging (no pre-treatment) during the reduction step.

*Stability* – The experimental setup for multiple cycling is schematically shown in Figure S4. The furnace (VHT-E48, Ulvac-Riko) consists of four electric heating elements surrounded by gold-coated refrigerated mirrors to direct IR radiation towards the centerline. A 1.6 g RPC sample was placed inside a 24 mm-outer diameter, 1.5 mm-thickness, 500 mm-length quartz tube. Temperature was measured using a B-type thermocouple. Argon (99.996% purity) and synthetic air flow rates were regulated with electronic mass flow controllers (Bronkhorst, EL-FLOW). Steam flow rate

---

\* Corresponding author. Email: [aldo.steinfeld@ethz.ch](mailto:aldo.steinfeld@ethz.ch)

was controlled by a liquid flow meter (Bronkhorst, Liqui-Flow) connected to an evaporator (Bronkhorst, Controlled Evaporator Mixer,  $T = 175\text{ }^{\circ}\text{C}$ ). Oxygen evolution during reduction was analyzed with a calibrated mass spectrometer (GSD 320, Pfeiffer Vacuum). To initiate the redox cycle, the RPC sample was heated to the reduction temperature  $T_{\text{reduction}} = 1500\text{ }^{\circ}\text{C}$  at a heating rate  $600\text{ }^{\circ}\text{C min}^{-1}$  while flowing Ar at a rate  $\dot{V}_{\text{Ar}} = 0.3\text{ L min}^{-1}$ . Reduction was continued isothermally at  $T_{\text{reduction}}$  for 3.5 min. The sample was then cooled to  $T_{\text{oxidation}} = 600\text{ }^{\circ}\text{C}$  at a cooling rate  $600\text{ }^{\circ}\text{C min}^{-1}$ . Oxidation was performed isothermally at  $T_{\text{oxidation}}$  for 5 min. with a mixture of steam and Ar at flow rates of 0.15 and  $0.3\text{ L min}^{-1}$ , respectively. To ensure full oxidation, the sample was subsequently oxidized for additional 0.5 min with a mixture of synthetic air and Ar at flow rates of 0.15 and  $0.15\text{ L min}^{-1}$ , respectively. The cycle was then repeated. For these experimental conditions,  $\delta_{\text{red}} - \delta_{\text{ox}} = 0.031$ . Figure S5 shows the specific yield of  $\text{O}_2$  as a function of the cycle number for 500 consecutive redox cycles. Figure S6 presents scanning electron micrographs (SEM) of the strut's porosity of the RPC sample before and after the 500 consecutive redox cycles of Fig. S7.

*Energy efficiency* – The solar-to-fuel energy efficiency  $\eta_{\text{solar-to-fuel}}$  is defined as:

$$\eta_{\text{solar-to-fuel}} = \frac{Q_{\text{fuel}}}{Q_{\text{input}}} = \frac{Q_{\text{fuel}}}{Q_{\text{solar}} + Q_{\text{pump}} + Q_{\text{inert}}} \quad (1)$$

$Q_{\text{fuel}}$  is the energy content in the fuel (CO) produced, given by:

$$Q_{\text{fuel}} = \Delta H_{\text{fuel}} \int r_{\text{fuel}} dt \quad (S2)$$

where  $\Delta H_{\text{fuel}}$  is the molar heating value of CO produced ( $\Delta H_{\text{fuel}} = 283\text{ kJ/mol}$ ) and  $\int r_{\text{fuel}} dt$  is the measured molar rate of CO produced integrated over the duration of the oxidation step.  $Q_{\text{solar}}$  is the total solar energy input integrated over the duration of the reduction step:

$$Q_{\text{solar}} = \int P_{\text{solar}} dt \quad (\text{S3})$$

where  $P_{\text{solar}}$  is the measured radiative power input through the solar reactor's aperture, accounting for the measured 93.2% total transmittance of the quartz window<sup>1</sup>.  $Q_{\text{pump}}$  and  $Q_{\text{inert}}$  are the energy penalties associated with vacuum pumping and inert gas consumption during the reduction step.  $Q_{\text{pump}}$  is calculated as the thermodynamic minimum pumping work divided by the product of two efficiencies, namely the heat-to-work efficiency  $\eta_{\text{heat-to-work}}$  (assumed 0.4) and the vacuum pump efficiency  $\eta_{\text{pump}}$ , according to:

$$Q_{\text{pump}} = \frac{1}{\eta_{\text{heat-to-work}} \cdot \eta_{\text{pump}}} \int \dot{n}(t) \cdot R \cdot T \cdot \ln \left( \frac{P_{\text{atmospheric}}}{P_{\text{reactor}}(t)} \right) dt \quad (\text{S4})$$

where  $\dot{n}(t)$  is the sum of the measured molar flow rates of Ar gas injected and O<sub>2</sub> released by ceria during the reduction step. The pump efficiency for a multi-stage industrial arrangement is given by:

$$\eta_{\text{pump}} = 0.07 \cdot \log \left( \frac{P_{\text{total}}}{P_{\text{atmospheric}}} \right) + 0.4 \quad (\text{S5})$$

where  $p_{\text{total}}$  is the measured total pressure inside the cavity. Note that  $\eta_{\text{solar-to-fuel}}$  is weakly depended on  $\eta_{\text{pump}}$  because  $Q_{\text{solar}} \gg Q_{\text{pump}}$  at the moderate vacuum pressure levels applied during reduction in the range 10-1000 mbar. The energy required for inert gas separation is given by:

$$Q_{\text{inert}} = \frac{1}{\eta_{\text{heat-to-work}}} E_{\text{inert}} \int r_{\text{inert}} dt \quad (\text{S6})$$

where  $r_{\text{inert}}$  is the measured Ar gas flow rate during reduction and  $E_{\text{inert}}$  is the work required for inert gas separation, assumed 20 kJ per mole<sup>2</sup>. Re-radiation losses were calculated according to:

$$Q_{\text{rerad}} = \int_0^t \varepsilon_{\text{apparent}} A_{\text{aperture}} \sigma T(t)^4 dt \quad (\text{S7})$$

where  $\sigma$  is the Stefan-Boltzmann constant,  $T(t)$  is the measured nominal reactor temperature,  $A_{\text{aperture}}$  is the aperture area, and  $\varepsilon_{\text{apparent}}$  is the apparent emissivity of the cavity, assumed unity based on Monte Carlo ray tracing simulations. The energy required for the reduction of ceria was calculated using the measured amount of oxygen evolved and the enthalpy change of 475 kJ per mole of atomic oxygen<sup>4,5</sup>. For the sensible heating of ceria, a heat capacity of 83 J mol<sup>-1</sup> K<sup>-1</sup> was used<sup>9</sup>. Convection losses were calculated using Nusselt correlations for natural convection with the measured metallic shell temperatures<sup>6,7</sup>.

## Nomenclature

$A_{\text{aperture}}$  = aperture surface area

$E_{\text{inert}}$  = energy required for inert gas separation

$P_{\text{solar}}$  = solar radiative power input

$p$  = pressure

$r_{\text{fuel}}$  = molar rate of fuel (CO) production

$r_{\text{inert}}$  = inert gas flow rate

$T_{\text{reduction}}$  = maximum temperature during the reduction step

$T_{\text{oxidation,start}}$  = temperature at the beginning of the oxidation step

$T_{\text{oxidation,end}}$  = temperature at the end of the oxidation step

$R$  = universal gas constant

$\varepsilon_{\text{apparent}}$  = apparent emissivity of cavity

$\sigma$  = Stefan-Boltzmann constant

$t$  = time duration

$\delta$  = nonstoichiometry

$\Delta H_{\text{fuel}}$  = heating value of the fuel

$\eta_{\text{heat-to-work}}$  = heat-to-work efficiency

$\eta_{\text{pump}}$  = vacuum pump efficiency

$\eta_{\text{solar-to-fuel}}$  = solar-to-fuel energy efficiency

$\dot{V}$  = volumetric flow rate

$Q_{\text{inert}}$  = heat equivalent of work required for inert gas separation

$Q_{\text{input}}$  = total thermal energy input ( $Q_{\text{input}} = Q_{\text{solar}} + Q_{\text{inert}} + Q_{\text{pump}}$ )

$Q_{\text{pump}}$  = heat equivalent of work required for vacuum pumping

$Q_{\text{rerad}}$  = re-radiation losses through the cavity aperture

$Q_{\text{solar}}$  = solar radiative energy input

$Q_{\text{fuel}}$  = heating value of fuel produced

## Abbreviations

CPC compound parabolic concentrator

CSP concentrated solar power

DNI direct normal solar irradiation

L standard liters (at 273.15 K and 1 atm)

RPC reticulated porous ceramic

SEM scanning electron micrograph

## Bibliography

1. W. Villasmil *et al.*, *Journal of Solar Energy Engineering*, 2013, 136, 010901-010901.
2. Haring, H. W. *Industrial Gases Processing*, Wiley-VCH, 2008.
3. R. J. Panlener *et al.*, *Journal of Physics and Chemistry of Solids*, 1975, 36, 1213 - 1222.
4. M. Takacs *et al.*, *Physical Chemistry Chemical Physics*, 2015, 17, 7813-7822.
5. Touloukian, Y. S. *Thermophysical Properties of High Temperature Solid Materials. Volume 4. Oxides and Their Solutions and Mixtures. Part I. Simple Oxygen Compounds and Their Mixtures*, DTIC Document, 1966.
6. S. W. Churchill and H. H. S.Chu, *Journal of Heat and Mass Transfer*, 1975, 18, 1049-1053.
7. S. W. Churchill and H. H. S.Chu, *International Journal of Heat and Mass Transfer*, 1975, 18, 1323-1329.

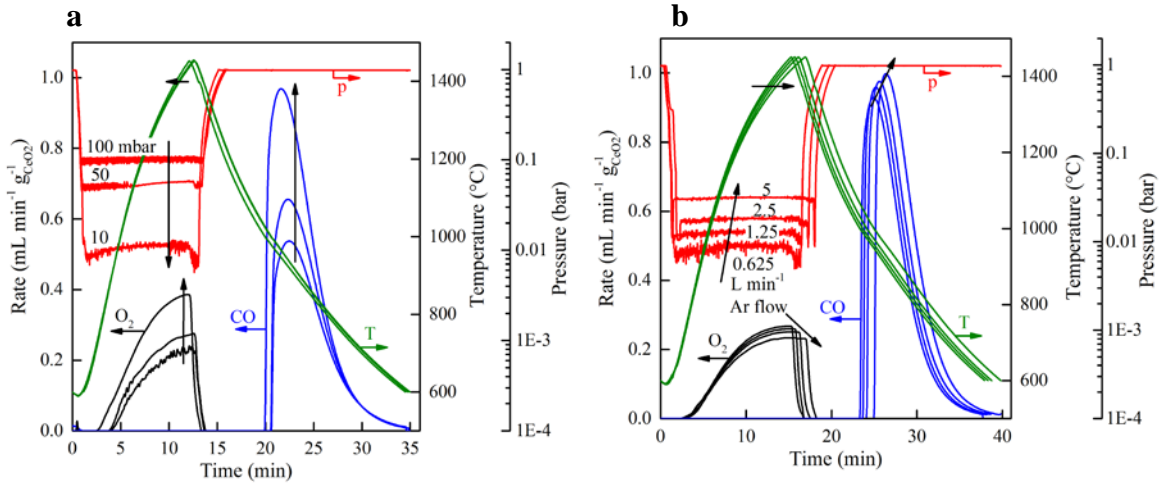


**Figure S1.** CO<sub>2</sub>-splitting cycles for various pressures and purge gas flow rates. Nominal solar reactor temperature, total pressure, and specific O<sub>2</sub> and CO evolution rates during CO<sub>2</sub>-splitting redox cycles, with the reduction step conducted under: a, varying  $p_{\text{total}}$ , and b, varying  $\dot{V}_{\text{Ar}}$ . Black arrows indicate the trends for increasing  $\dot{V}_{\text{Ar}}$  (a) and decreasing  $p_{\text{total}}$  (b). Experimental conditions during reduction for cycles of Fig. S1a:  $P_{\text{solar}} = 3.5 \text{ kW}$ ,  $T_{\text{reduction}} = 1450 \text{ }^\circ\text{C}$ ,  $\dot{V}_{\text{Ar}} = 0.625 \text{ L min}^{-1}$ , and  $p_{\text{total}} = 10, 50, \text{ and } 100 \text{ mbar}$ . Experimental conditions during reduction for cycles of Fig. S1b:  $P_{\text{solar}} = 2.9 \text{ kW}$ ,  $T_{\text{reduction}} = 1450 \text{ }^\circ\text{C}$ ,  $p_{\text{total}} = 10\text{-}20 \text{ mbar}$ , and  $\dot{V}_{\text{Ar}} = 0.625, 1.25, 2.5 \text{ and } 5 \text{ L min}^{-1}$ . Experimental conditions during oxidation for cycles of Figs. S1a and S1b:  $P_{\text{solar}} = 0 \text{ kW}$ ,  $T_{\text{oxidation,start}} = 1000 \text{ }^\circ\text{C}$ ,  $\dot{V}_{\text{CO}_2} = 7 \text{ L min}^{-1}$ , and  $p_{\text{total}} = 1 \text{ bar}$ .

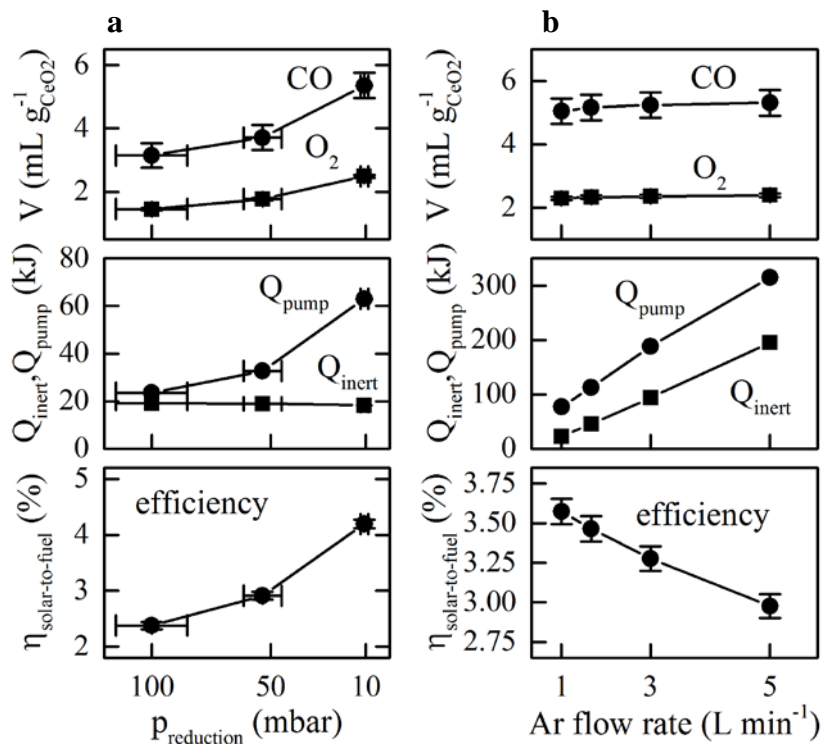


**Figure S2.** Performance indicators for various pressures and purge gas flow rates. Absolute O<sub>2</sub>/CO evolution, energy required for inert gas separation and vacuum pumping, and solar-to-fuel energy efficiency as a function of: a, the total pressure applied during the reduction step; and b, the Ar gas flow rate applied during the reduction step. Experimental conditions during reduction for S2a:  $P_{\text{solar}} = 3.5$  kW,  $T_{\text{reduction}} = 1450$  °C,  $\dot{V}_{\text{Ar}} = 0.625$  L min<sup>-1</sup> at  $p_{\text{total}} = 10, 50,$  and  $100$  mbar. Experimental conditions during reduction for S2b:  $P_{\text{solar}} = 2.9$  kW,  $T_{\text{reduction}} = 1450$  °C, and  $\dot{V}_{\text{Ar}} = 0.625, 1.25, 2.5,$  and  $5$  L/min at  $p_{\text{total}} = 10$  mbar. Experimental conditions during oxidation for S2a and S2b:  $P_{\text{solar}} = 0$  kW,  $T_{\text{oxidation,start}} = 1000$  °C,  $T_{\text{oxidation,end}} = 600$  °C, and  $\dot{V}_{\text{CO}_2} = 7$  L min<sup>-1</sup> at  $p_{\text{total}} = 1$  bar.

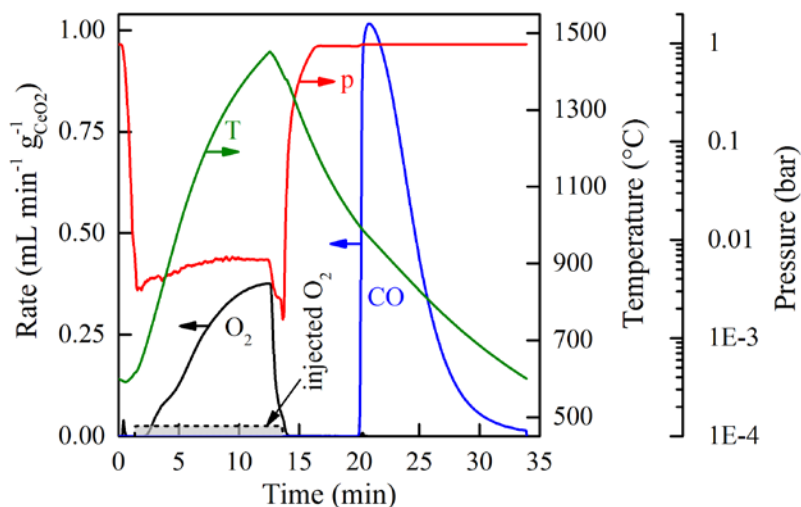


**Figure S3.** CO<sub>2</sub>-splitting cycle without inert gas. Nominal solar reactor temperature, total pressure, and specific O<sub>2</sub> and CO evolution rates for a CO<sub>2</sub>-splitting cycle with ambient air purging during the reduction step. The dashed line indicates the rate of O<sub>2</sub> injected with the air. Experimental conditions during reduction:  $P_{\text{solar}} = 3.5 \text{ kW}$ ,  $T_{\text{reduction}} = 1450 \text{ }^{\circ}\text{C}$ ,  $p_{\text{total}} = 10\text{mbar}$ , and  $\dot{V}_{\text{air}} = 0.2 \text{ L min}^{-1}$ . Experimental conditions during oxidation:  $P_{\text{solar}} = 0 \text{ kW}$ ,  $T_{\text{oxidation,start}} = 1000 \text{ }^{\circ}\text{C}$ ,  $p_{\text{total}} = 1 \text{ bar}$ , and  $\dot{V}_{\text{CO}_2} = 7 \text{ L min}^{-1}$ .

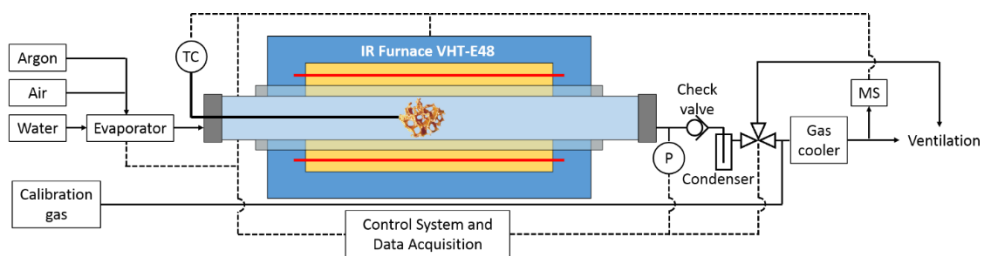


**Figure S4.** Schematic of the experimental setup for multiple cycling. The RPC sample is placed in a quartz tube enclosed by an IR furnace. Temperature is measured with a type-B thermocouple. Purge and oxidant gases are delivered with electronic mass flow controllers. Excess steam is condensed in a glass condenser and product gases are cooled in a gas cooler. The oxygen evolved during reduction is analyzed by a calibrated mass spectrometer.



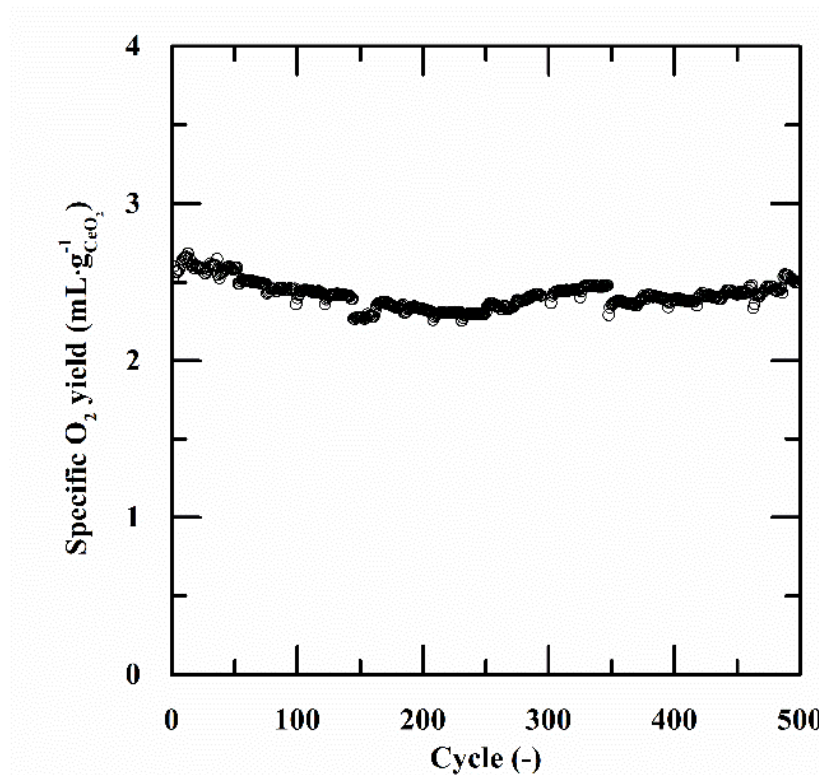


**Figure S5.** Material stability. Specific yield of O<sub>2</sub> for 500 consecutive redox cycles ( $\delta_{\text{red}} - \delta_{\text{ox}} = 0.031$ ). Experimental conditions: heating/cooling rate 600 °C min<sup>-1</sup>; reduction at  $T_{\text{reduction}} = 1500$  °C for 3.5 min with  $\dot{V}_{\text{Ar}} = 0.3$  L min<sup>-1</sup>; oxidation at  $T_{\text{oxidation}} = 600$  °C for 5 min with  $\dot{V}_{\text{H}_2\text{O}} = 0.15$  L min<sup>-1</sup> and  $\dot{V}_{\text{Ar}} = 0.3$  L min<sup>-1</sup> and for 0.5 min with  $\dot{V}_{\text{air}} = 0.15$  L min<sup>-1</sup> and  $\dot{V}_{\text{Ar}} = 0.15$  L min<sup>-1</sup>.

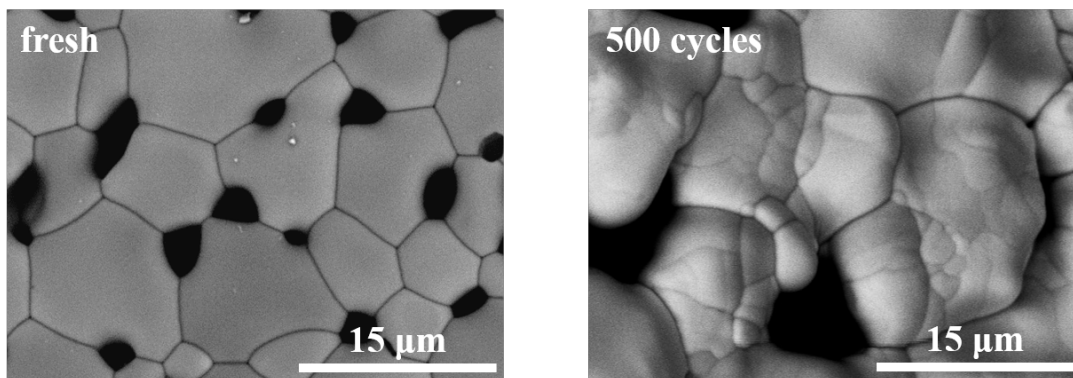


**Figure S6.** SEM of the RPC sample showing the strut's porosity before and after 500 consecutive redox cycles of Fig. S5.